POM/PU/Carbon Nanofiber Composites Produced by Water-Mediated Melt Compounding: Structure, Thermomechanical and Dielectrical Properties

S. Siengchin,[1,4] G. C. Psarras,[2] J. Karger-Kocsis[3]

[1]*Production Engineering Department, The Sirindhorn International Thai-German Graduate School of Engineering (TGGS), King Mongkut's University of Technology North Bangkok, Bangsue 10800, Bangkok, Thailand*
[2]*Department of Materials Science, School of Natural Sciences, University of Patras, Patras 26504, Greece*
[3]*Polymer Technology, Faculty of Engineering and the Built Environment, Tshwane University of Technology, Pretoria 0001, Republic of South Africa*
[4]*Research Center of Nano-Industries and Bio-Plastics, Science and Technology Research Institute, King Mongkut's University of Technology North Bangkok, Bangsue 10800, Bangkok, Thailand*

Received 20 November 2009; accepted 22 January 2010
DOI 10.1002/app.32133
Published online 29 March 2010 in Wiley InterScience (www.interscience.wiley.com).

ABSTRACT: Binary and ternary composites composed of polyoxymethylene (POM), polyurethane (PU), and carbon nanofiber (CNF) were produced by water-mediated melt compounding. PU latex and/or aqueous CNF dispersion were introduced into the molten POM in laboratory kneader to prepare toughened and/or nanoreinforced POM composites. The crystallization of the POM-based systems was studied by polarized optical microscopy. The dispersion of the CNF was inspected in scanning electron microscopy. The mechanical and thermomechanical properties of the composites were determined by dynamic-mechanical analysis, thermogravimetric analysis, short-time creep-, stress relaxation-, and uniaxial static tensile tests. The dielectric response of the nanocomposites was investigated by means of broadband dielectric spectroscopy at ambient temperature. CNF worked as reinforcement (i.e., increased the stiffness, resistance to creep, tensile strength, and reduced the elongation at break), and also improved the thermo-oxidative stability of POM. PU alone had an adverse effect to the above listed properties, which could be enhanced again by additional incorporation of CNF. Dielectric spectroscopy proved to be a useful tool to get deeper understanding on morphological changes caused by the additives. © 2010 Wiley Periodicals, Inc. J Appl Polym Sci 117: 1804–1812, 2010

Key words: nanocomposite; polymer blend; structure-property relationships; polyoxymethylene (POM); carbon nanofiber (CNF); toughening; polyurethane; latex

INTRODUCTION

Polyoxymethylene (POM) possesses some outstanding properties, such as easy processing, high stiffness and tensile strength, high heat deflection temperature, and solvent resistance.[1,2] Therefore, POM is widely used, especially in the automotive and electronic sectors. On the other hand, the application of POM is often limited because of its high crystallinity accompanied with brittleness and low-impact resistance (e.g., Refs. 3 and 4). To date, POM has been combined with polyurethane (PU), ethylene-propylene-diene terpolymer, and other rubbery materials to improve its toughness (e.g., Refs. 5 and 6). POM/PU blends, exhibiting high-impact strength and good thermal stability, are well established in the market. The PU additive is mostly a thermoplastic version that is incorporated into POM via melt compounding.

Nowadays, considerable interest is devoted to nanocomposites due to the attractive properties, which can be reached by adding nanofillers. POM/PU blends were already modified by nanoscaled fillers, including aluminum oxide,[7] and calcium carbonate,[8] to upgrade the mechanical and thermal properties. Unlike to carbon nanotubes (CNTs), very few research studies addressed the property improvements of polymers by adding carbon nanofibers (CNF). It has been shown that the dielectric and mechanical properties of polymer-based nanocomposites were markedly improved by the addition of CNF.[9,10] Similar to CNT, CNF has also a high-reinforcing efficiency. Its presence in a small amount in the corresponding polymer, typically less than 5 wt %, can result in significant improvement in mechanical properties. It has been reported that adequate interfacial adhesion of CNF to the related matrix and its uniform dispersion are the key factors in

Correspondence to: S. Siengchin (suchart.s.pe@tggs-bangkok.org).

respect to the reinforcing effect.[11] Being much longer than CNT, the disentanglement of CNF and its fine dispersion on polymers is a problematic issue. Accordingly, various methods, like in situ polymerization, solution blending have been tried to disperse CNF in polymers. On the other hand, aqueous CNF dispersions are also available. Their use offers several benefits: reduced health risk due to the water carrier, good dispersability owing to low CNF concentration, combination possibility with other aqueous-based systems (e.g., polymer latices). Note that the latex compounding is a very straightforward technique to produce impact-modified thermoplastics due to the fact that the mean particle size in latices is closely matched with the required size of the toughening agent (impact modifier). Provided that the particle size of the latex can be kept during the so-called water-mediated melt compounding, toughened thermoplastics can be produced online in a cost efficient way.[12] Water-mediated means that the water serves as a carrier to introduce the toughening agent and/or nanofiller into the melt of suitable polymers (being hydrolysis resistant) before the water is forced to evaporate in subsequent section of the extruder. This water-mediated compounding has been successfully adapted for POM-based systems (toughened and nanofilled).[13,14] As nanofillers water swellable layered silicate and water dispersible boehmite alumina particles were used.

The goal of this work was to explore further the potential of the water-mediated compounding using PU latex and/or aqueous CNF dispersion, and study the mechanical, thermal, and dielectric properties of the related composites. As matrix material POM has been chosen.

EXPERIMENTAL

Materials and preparation of composites

Aqueous dispersion of CNF with a concentration of 15 g/L was donated by Grupo Antolin (Burgos, Spain). The related CNF had a diameter range of 20–80 nm, a graphitization degree of about 70 wt %, and a metallic particle content of 6–8 wt %. Although the length of the CNFs from Grupo Antolin is usually greater than 30 μm, no information was available on the aspect ratio of the CNF aqueous dispersion delivered. PU latex with 50 wt % dry content (Acralen U 550) was kindly supplied by Polymer Latex GmbH (Marl, Germany). The size of the PU particles ranged from 100 to 1000 nm (according to suppliers' information). Granulated POM (Hostaform C 9021, Ticona GmbH, Frankfurt, Germany) was utilized as polymeric matrix for all composite systems. Its volumetric melt flow rate (MVR at 190°C/2.16 kg) was 8 cm^3/10 min.

TABLE I
Recipe and Designation of the POM-Based Systems

Sample designation	PU content (wt %)	CNF content (wt %)
POM	–	–
POM/PU(10)	10	–
POM/CNF(0.1)	–	0.1
POM/PU(10)/CNF(0.1)	10	0.1

POM/PU blend, POM/CNF binary, and POM/PU/CNF ternary nanocomposites were prepared by laboratory kneader (Type 50 of Brabender, Duisburg, Germany) at $T = 190$°C and rotor speed of 60 rpm. The PU rubber particle and/or CNF contents in the system investigated (blend, binary, and ternary composites) were set for 10 and 0.1 wt %, respectively. The aqueous dispersion of CNF and/or PU latex were dropped in the POM melt after its mastication for 2 min in the kneading chamber. The overall duration of the melt mixing for both binary and ternary nanocomposites was 6 min. The compounds were compression molded into 1-mm thick sheets at $T = 200$°C using a hot press (EP-Stanzteil, Wallenhorst, Germany). The composition and designation of the compounds studied are given in Table I.

Characterization and testing

Crystallization and melting properties

The spherulite growth was observed by polarized light microscopy (PLM). Samples were isothermally crystallized in a hot stage (THMS 600/S, Raczek Analysentechnik, Wedemark, Germany). Thin films of the materials with a thickness of 20–30 micron were used. The film was melted at 200°C for 1 min and then cooled to the isothermal crystallization temperature ($T = 148$°C) where it was hold for 60 min.

Differential scanning calorimetry (DSC) traces were recorded on a Mettler DSC 821 device (Mettler-Toledo, Giessen, Germany) in the temperature range from −100°C to 200°C at a heating and cooling rate of 10°C/min. The crystallinity (X_c) of POM was calculated from the following equation:

$$X_c = \frac{\Delta H_m}{\Delta H_m^0} 100\% \quad (1)$$

where ΔH_m is the melt enthalpy of the POM in the sample (net POM content considered), ΔH_{m}^0 is the melt enthalpy of POM with 100% crystallinity ($X_c = 100\%$) for which 186 J/g was taken, as reported in Ref. 8.

Thermal and thermomechanical properties

Thermogravimetric analysis (TGA) was performed on a TG50 Mettler-Toledo device. TGA experiments

were conducted in the temperature range from 25 to 600°C under oxygen flushing at a heating rate of 10°C/min and the weight loss was monitored.

Dynamic-mechanical analysis (DMA) was made in tensile mode at 1 Hz frequency using a DMA Q800 apparatus (TA Instruments, New Castle, NJ). The storage moduli (E') along with mechanical loss factor (tan δ) were determined as a function of the temperature ($T = -100°C...+150°C$). The strain applied was 0.1% and the heating rate was set for 3°C/min. The specimen was a dumbbell-shaped type (S3A according to DIN 53504).

Creep and tensile response

Short-time creep and stress relaxation tests were made in tensile mode at different temperatures using the above DMA apparatus. The creep- and recoverable compliance were determined as a function of the time ($t_{creep} = 60$ min and $t_{recovery} = 120$ min). The applied tensile stress was 6 MPa (at 0.35% strain). This value was derived from a test series checking the presence of linear isochronous deformation. The relaxation modulus was determined as a function of the time ($t_{relax} = 90$ min). The applied tensile strain was 1%. The creep and stress relaxation tests were performed on dumbbell-shaped specimens (5B type according to DIN-EN ISO 527) by considering their rectangular section.

Tensile tests were performed on dumbbell-shaped specimens (DIN-ISO-527) in a Zwick 1474 (Ulm, Germany) universal testing machine. Tests were run at room temperature at $v = 2$ mm/min crosshead speed and the related stress–strain curves were registered.

Morphology detection

The dispersion of CNF in the POM nanocomposites was studied by scanning electron microscopy (SEM) technique. The fracture surfaces of tensile loaded specimens were subjected to SEM inspection in a Supra™ 40VP SEM (Carl Zeiss GmbH, Oberkochen, Germany). The surface was carbon coated prior to SEM inspection performed at low-acceleration voltage.

Dielectric response

Broadband dielectric measurements were performed in the frequency range of 10^{-3} to 10^{6} Hz, by means of Alpha-N Frequency Analyzer, supplied by Novocontrol Technologies GmbH (Hundsangen, Germany) at room temperature. The employed test cell was a two electrodes gold-coated plate capacitor, BDS 1200, supplied also by Novocontrol, which was suitably shielded.

RESULTS AND DISCUSSION

Morphology

The spherulite size can play an important role in improving the mechanical properties of polymer composites.[8,15] The effects of PU and CNF on the morphology of POM systems are displayed in Figure 1. During crystallization POM produced large spherulites of about 100–150 μm diameter. Incorporation of CNF reduced the mean size of the spherulites suggesting its nucleation effect. The spherulite size of the POM/PU/CNF ternary composite was the lowest of all systems (ca. 30–70 μm). It is noteworthy, that the addition of PU significantly disturbs the spherulitic structure of POM. POM/PU/CNF composite exhibited a finer spherulite structure than the POM/PU blend. Apart of effects on the spherulite structure, it has been reported that incorporation of CNF increases the crystallinity of POM.[9] This is in concert with our DSC observation. The incorporation of PU and PU/CNF influenced slightly the crystallinity of POM in the related systems—compare DSC data summarized in Table II. It was found that both the melting (T_m) and crystallization temperature (T_c) of the composites containing 0.1 wt % CNF increased slightly compared with the neat POM.

Thermo-oxidative properties

Figure 2 shows the weight loss versus T traces for the POM, POM/PU blend, POM/CNF binary, and POM/PU/CNF ternary composites. Note that the thermal degradation of the neat POM is a one-step procedure representing depolymerization. Incorporation of PU reduces slightly, whereas CNF markedly the onset of the thermal degradation. The follow-up degradation of the POM/CNF runs, however, at higher temperature than both POM and POM/PU blend. The POM/PU/CNF ternary composite has the highest onset decomposition temperature. Moreover, the related mass loss versus temperature trace is parallel shifted to that of the POM toward higher temperatures. Accordingly, the common use of PU and CNF resulted in a synergistic effect in the thermo-oxidative stability of POM.

DMA response

DMA spectra in form of storage modulus (E') and loss factor (tan δ) as function of temperature (T) are demonstrated in Figure 3(a,b), respectively. One can notice that the stiffness values of the POM/CNF composite were slightly higher than that of the neat POM in the whole temperature range. This indicates the reinforcing effect of CNF. As expected, adding PU rubber was associated with a drop in the storage modulus of the POM/PU blend compared with the

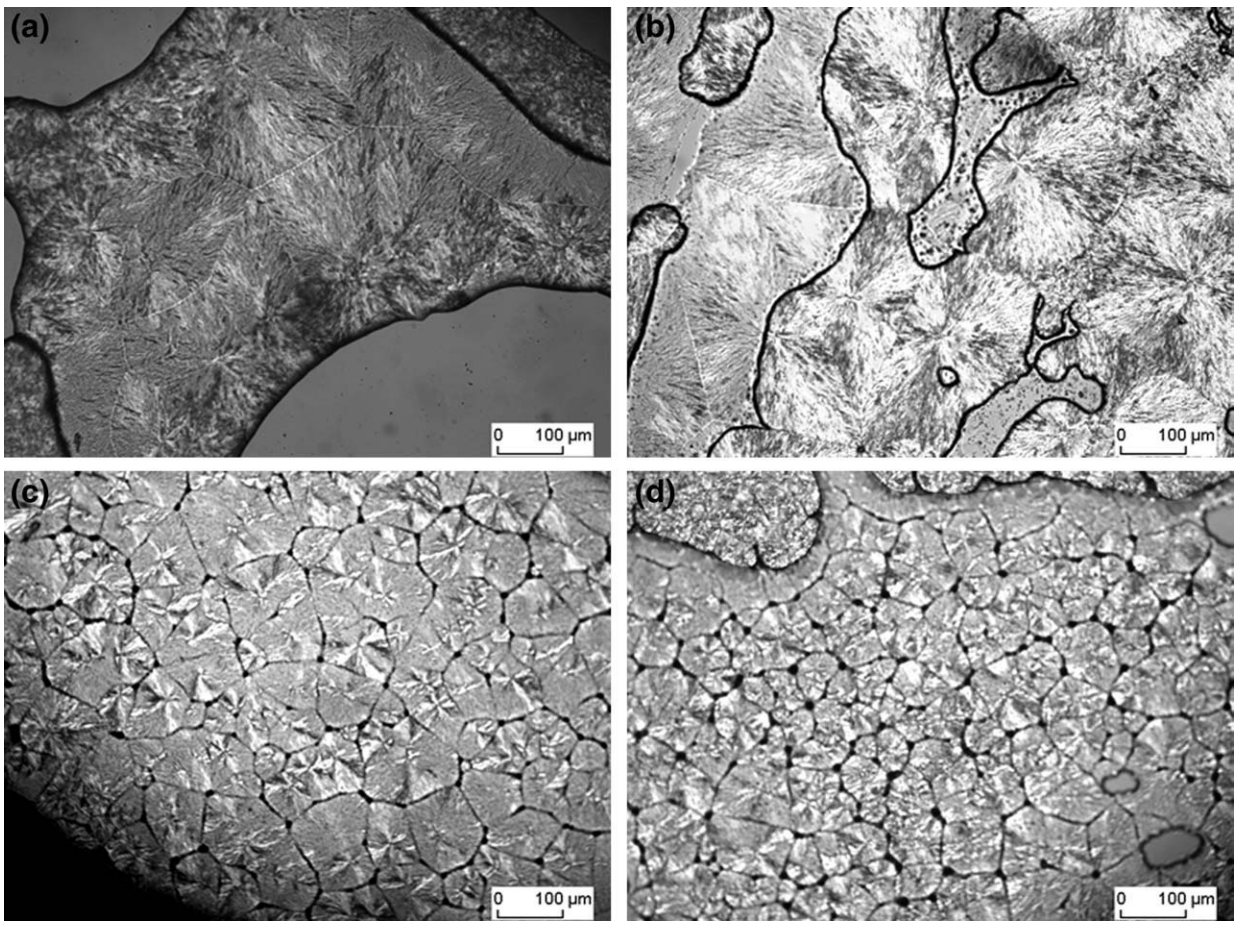

Figure 1 PLM pictures of the isothermally (T = 148°C) crystallized POM (a), POM/PU blend (b), POM/CNF (c), and POM/PU/CNF (d).

neat POM. The storage modulus versus T curves of the POM/PU and POM/PU/CNF systems were practically the same. The plots in Figure 3(b) reveal three relaxation transitions in POM. The glass transition temperature (T_g) is located at around −60°C (γ-relaxation transition). Another two peaks, observed at about −2°C and about 130°C correspond to the β- and α-relaxations, respectively. These relaxation processes are assigned to the motions of long molecular segments in disordered (β) and well-ordered crystalline phases (α), respectively.[16] Incorporation of PU yielded an additional maximum peak at about −50°C in the tan δ versus T trace, which represents the T_g of the PU component. Adding CNF and/or PU was accompanied with a shift in both the α- and β-relaxations to lower temperatures (ca. 5°C). This finding is somewhat at odds with the DSC results showing similar crystallinities (cf. Table II). One possible explanation is that small agglomerates of CNF and matrix voids within this network support the movement of macromolecular chains yielding a small reduction in the T_g (β-relaxation) of the matrix.[17] To figure out the possible reason for the observed change in the α-relaxation further investigations are needed.

Based on SEM results, the mean particle size of the PU domains was about 2 µm in the POM/PU and POM/PU/CNF. This is larger than the size of

TABLE II
Crystallization and Melting Characteristics of the Systems Studied

Sample designation	T_m (°C)	T_c (°C)	Delta H_m (J/g)	% X_c (POM)
POM	166.8	145.9	155.2	83.4
POM/PU(10)	168.7	145.5	156.3	84.0
POM/CNF(0.1)	168.1	146.1	158.1	85.0
POM/PU(10)/CNF(0.1)	169.3	145.7	158.3	85.1

T_m, melting temperature; T_c, crystallization temperature; H_m, melting enthalpy; X_c, crystallinity (based on the net POM content).

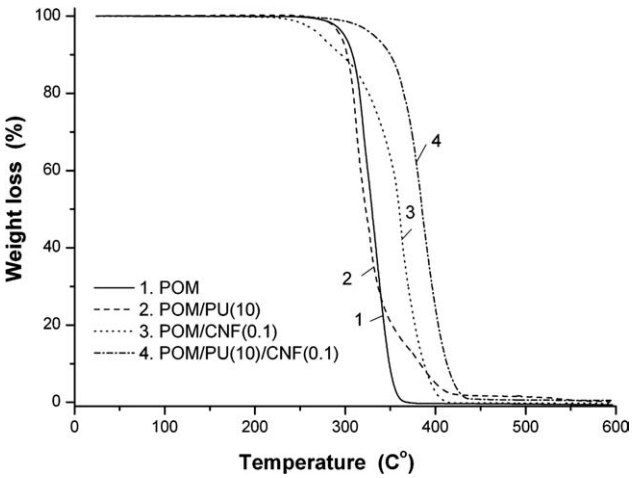

Figure 2 Weight loss versus temperature for the POM, POM/PU, POM/CNF, and POM/PU/CNF.

the primary PU particles in the related latex, agrees, on the other hand, with the findings in our former works using this water-mediated melt compounding for similar POM/PU systems.[7,14] It will be disclosed later that average length of CNF was about 6 μm in the related systems. This suggests that CNF should work as reinforcement in the POM matrix even in the POM/PU blend. However, this was not obvious in the DMA spectra in Figure 3(a). Therefore, creep tests were performed to check the reinforcing effect of CNF.

Creep and creep recovery

Figures 4 and 5 demonstrate the effects of CNF and PU incorporations on the creep and creep recovery responses of POM, respectively. Introducing CNF into POM resulted in a considerable reduction in the creep as shown by the plots of creep and recovered creep compliances versus time (cf. Figs. 4 and 5, respectively). Accordingly, CNF acts as reinforcing phase in POM. This finding is in accordance with the DMA results [cf. Fig. 3(a)]. The presence of PU rubber particles increases the creep and creep recovery compliance data. This is again in line with the expectation based on the DMA spectra [cf. Fig. 3(a)]. Additional incorporation of CNF into the POM/PU blend improves, however, the resistance to creep (cf. Figs. 4 and 5) confirming the reinforcing action of CNF also in this blend. This suggests that CNF is located in the POM rather than in the PU phase, and in addition, it is finely dispersed. The latter is reasoned by the fact, that CNF was introduced from a highly dilute suspension (CNF concentration ca. 1.5 wt %) during the water-mediated melt compounding process. It is noteworthy that the creep response is a better indicator of the CNF reinforcement than the

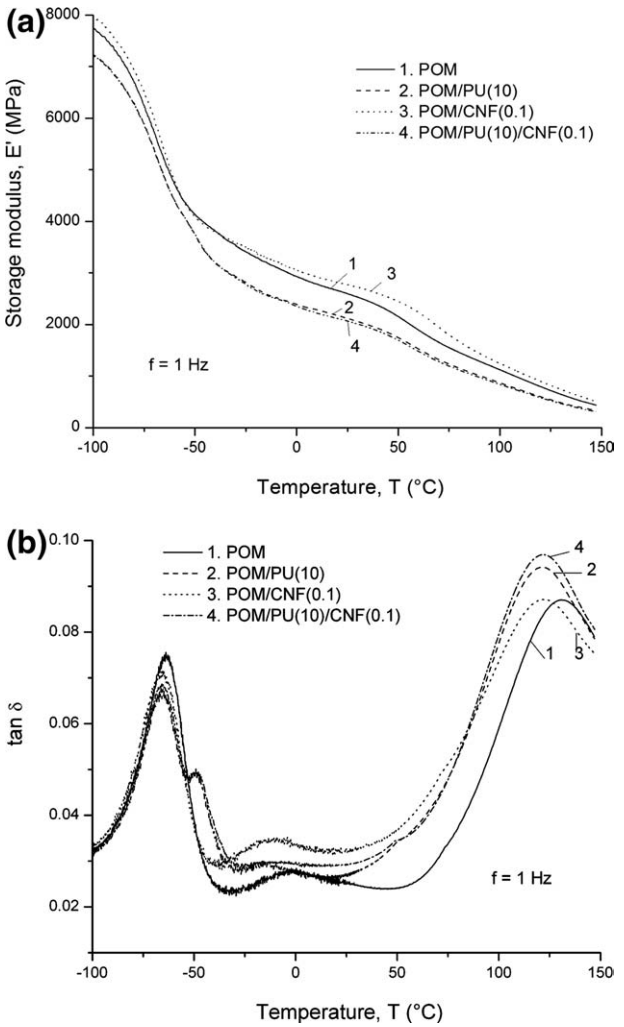

Figure 3 (a) E' versus T and (b) tan δ versus T traces for the POM, POM/PU blend, POM/CNF binary, and POM/PU/CNF ternary composites.

storage modulus in DMA [compare the difference in the related curves in Figs. 4 and 5 and in Fig. 3(a)].

Stress relaxation

Figure 6 displays the traces of the relaxation modulus as a function of time for the POM, POM/PU blend and the CNF-containing binary-, and ternary composites. The shape of the relaxation curves of the systems is similar to that of the neat POM. However, their relaxation modulus decreased remarkably with incorporation of PU compared with the neat POM. One can see that the relaxation modulus of the POM/CNF binary composite is higher in the whole relaxation time range than those of the POM (but only slightly), POM/PU blend and POM/PU/CNF ternary composite (the latter two are closely matched). The increase of the relaxation modulus with the CNF presence is due to its reinforcing effects. Note that the long CNFs (mean length of ca.

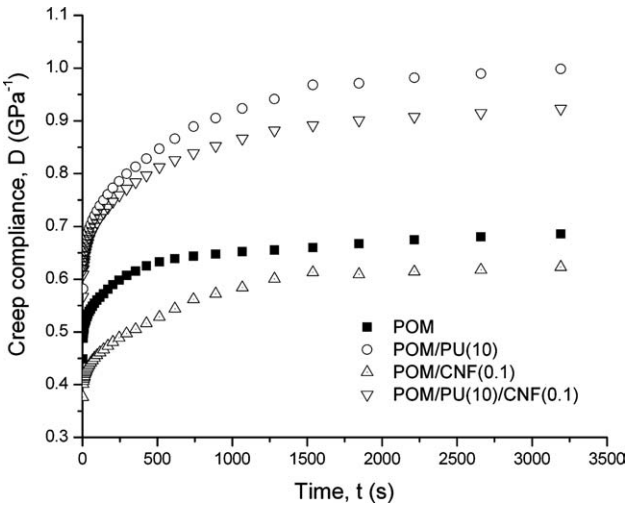

Figure 4 Creep of the POM, POM/PU blend and POM/CNF binary and POM/PU/CNF ternary composites at $T = 30°C$. Note: stress applied for $t = 60$ min.

6 μm, as disclosed later) may relieve very efficiently such stress concentration effects which are induced by material heterogeneities. This finding is coherent with those deduced from creep (cf. Figs. 4 and 5), DMA [cf. Fig. 3(a)] and tensile mechanical tests (cf. Fig. 7).

Tensile tests

The effects of CNF and PU on the tensile mechanical data are shown in Figure 7. The enhancement in tensile strength of nanocomposites containing 0.1 wt % CNF was about 18% compared with the neat POM. The primary reason for that is that due to the uniform dispersion of CNF in POM, an efficient load transfer occurs from the matrix toward the CNF.

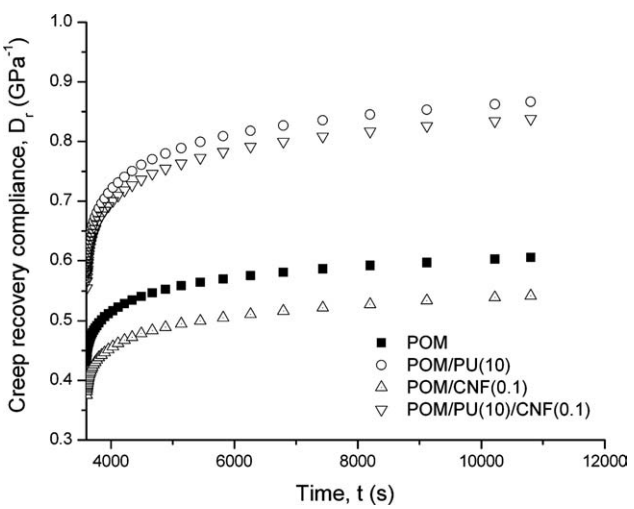

Figure 5 Creep recovery of the POM, POM/PU blend and POM/CNF binary and POM/PU/CNF ternary composites at $T = 30°C$. Note: stress removal at $t = 60$ min.

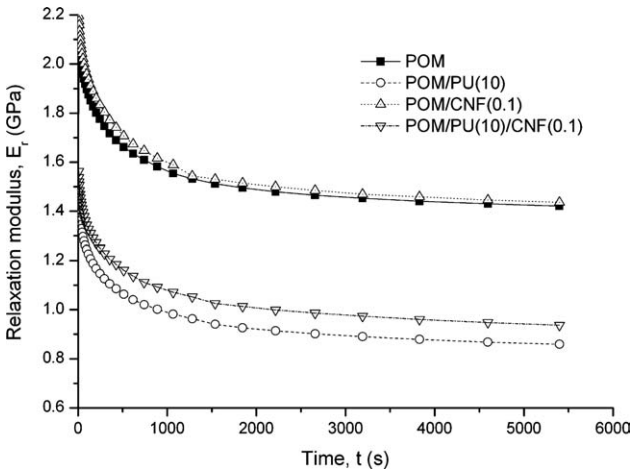

Figure 6 Relaxation modulus of the POM, POM/PU blend, POM/CNF binary and POM/PU/CNF ternary composites.

SEM picture also confirms that the CNF is well dispersed in POM matrix (cf. Fig. 8). Although the authors have only SEM evidence for that, a fine CNF dispersion is expected already based on the low concentration of CNF in the aqueous suspension used. SEM pictures taken from the fracture surfaces of the specimens indicated that the residual mean length of CNF is about 6 μm. Note that a reinforcing effect is generally accompanied with reduced ductility in all composite materials. This is the case also for the POM/CNF nanocomposite the elongation at break value of which is below that of the neat POM. Introducing PU has an adverse effect: the tensile strength decreases, whereas the elongation at break increases markedly. Note that this is the usual response of thermoplastics with impact modifier under static loading conditions. Additional incorporation of CNF increases the tensile strength and reduces the elongation at break of the POM/PU

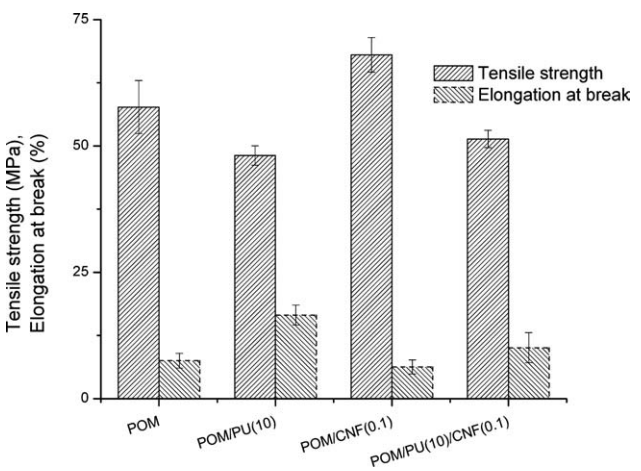

Figure 7 Tensile mechanical characteristics of the systems studied.

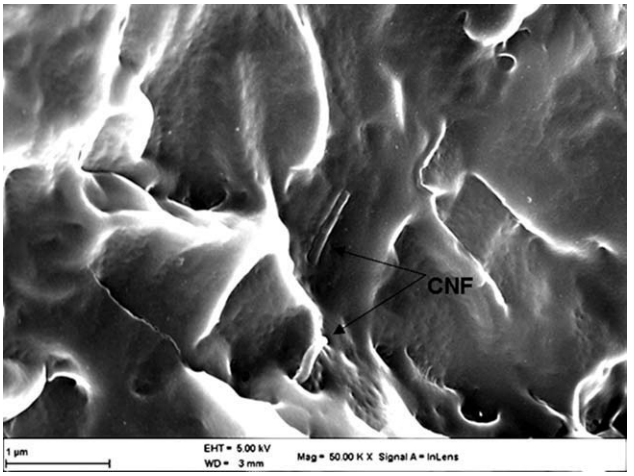

Figure 8 SEM picture taken from POM/CNF composite. Note: Arrow indicates CNF.

blend confirming that CNF acts as reinforcement also here (cf. Fig. 7).

Dielectric response

Dielectric spectroscopy is a powerful experimental tool for the investigation of polarization and conductivity mechanisms, molecular mobility, phase changes, and interfacial phenomena in polymers and polymer matrix composites. Experimental data can be analyzed by means of different formalisms, such as dielectric permittivity, ac conductivity, and electric modulus formalism. Although the recorded electrical effects can be described and analyzed in terms of any of the aforementioned formalisms, under certain conditions a specific formalism could be proved more helpful in extracting information with respect to the occurring physical processes. Electric modulus presentation exhibits some advantages in the interpretation of slow relaxation phenomena (processes with relatively enhanced relaxation time) in complex systems, mainly because of the elimination of the undesirable effect of electrode polarization.[18,19]

Electric modulus is defined as the inverse quantity of complex permittivity by the following equation:

$$M^* = \frac{1}{\varepsilon^*} = \frac{1}{\varepsilon' - j\varepsilon''} = \frac{\varepsilon'}{\varepsilon'^2 + \varepsilon''^2} + j\frac{\varepsilon''}{\varepsilon'^2 + \varepsilon''^2} = M' + jM'' \quad (2)$$

where ε' and M', and ε'' and M'' are the real the imaginary part of dielectric permittivity and electric modulus, respectively.

Figure 9(a) depicts the real part of electric modulus (M') as a function of frequency for POM, POM/PU blend, and the POM/CNF binary- and POM/PU/CNF ternary composites. The real part of electric modulus (M') as a function of frequency undergoes a step-like transition from low to high values for POM and POM/CNF binary composite. On other hand, the POM/PU blend and the POM/PU/CNF ternary composite exhibit, at least, two step-like transitions. These transitions correspond to relaxation processes, which become evident in the loss modulus index versus frequency plots.

Figure 9(b) depicts the dielectric spectra of the imaginary part of electric modulus (M'') as a function of the frequency of the applied field. In the case of pure POM, a single loss peak is recorded in the low frequency region, which is assigned as α-relaxation. According to the DMA results, three relaxation modes are expected to occur in the POM spectrum. However, at room temperature, and in the examined frequency range only the slower transition is recorded. The origin of this process cannot be ascribed undisputedly. It has been attributed to rearrangements in the crystalline parts of POM,

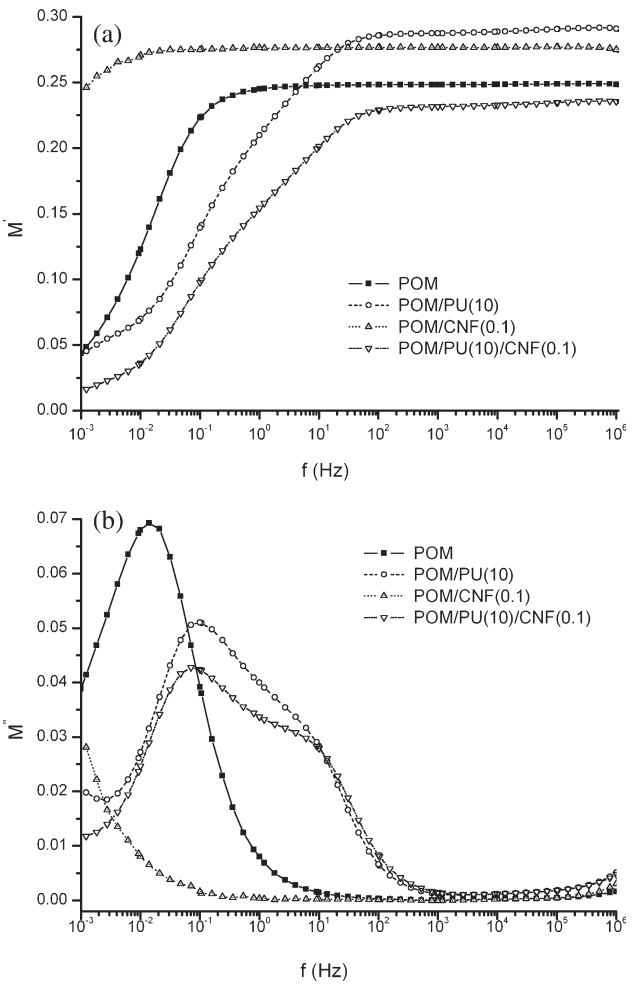

Figure 9 Real (a) and imaginary (b) part of electric modulus (M') versus frequency traces for the POM, POM/PU blend, POM/CNF binary, and POM/PU/CNF ternary composites.

although contributions from the amorphous phase cannot be excluded.[7,20,21] Since this is the slower occurring relaxation process in POM, it is reasonable to suggest that is related to interfacial polarization phenomena between crystalline and amorphous phases. Interfacial polarization (IP) occurs in heterogeneous and complex systems because of the accumulation of unbounded charges at the interfaces of the phases. The corresponding peak of POM/CNF system is not recorded in the examined frequency range, and it seems that is shifted to lower frequencies [cf. Fig. 9(b)]. This is a typical behavior for composite systems, where the presence of the reinforcing phase enhances heterogeneity, interfacial polarization (IP), and the relative relaxation time.[22,23] The situation differs in the case of POM/PU blend and the ternary system POM/PU/CNF. In their dielectric spectra two relaxation processes are recorded in the intermediate frequency region, while the tendency for the formation of a third peak is present in the high-frequency edge. From previous studies,[7,24,25] it is known that PU, at ambient, has a peak in the vicinity of 100 Hz (not shown here), related to its glass to rubber transition, and tends to form a second one at high frequencies. The latter is attributed to reorientation of polar side groups of the main chain.[25] Systems containing PU exhibit the aforementioned loss peaks. However, the third peak (the slower process) recorded close to 0.1 Hz cannot be connected with PU, and thus it should be assigned to POM. The peak locus of POM's α-mode appears to shift to higher frequencies by almost an order of magnitude in the POM/PU and POM/PU/CNF systems, indicating that the processes became faster. This is in qualitative agreement with the DMA results of Figure 3(b). In DMA traces, the high-temperature peaks of tan δ (α-mode) of POM/PU and POM/PU/CNF systems shift to lower temperatures with respect to POM denoting shorter relaxation times or faster relaxation processes.

The dielectric response of the examined systems is influenced by their variations in morphology. As it is already stated, the presence of PU affects the morphology of POM by disturbing the spherulitic structure of the latter. The extent of rigid crystalline regions is diminishing, rearrangement of crystallites and/or relaxation of isolated amorphous segments is facilitated and thus the peak of α-mode shifts to higher frequencies. Moreover, the incorporation of CNF reduces further the size of spherulites and consequently increases the interfacial area between the constituents and phases of the nanocomposite. The presence of CNF in the ternary system slightly influences the position of the peak by shifting to lower frequency, and at the same time reduces the intensity of electric modulus loss index (M″). In the dielectric permittivity formalism, enhanced heterogeneity and extensive interfacial area yield to increased values of the real and imaginary part of permittivity (ε′) and (ε″), respectively, at low frequencies. Recalling eq. (2), it should be noted that the same data expressed in the electric modulus formalism would provide reducing values of the real and imaginary part of electric modulus (M′) and (M″), respectively, with the increase of heterogeneity and interfacial area. Under this point of view, it is reasonable to suggest that the specific relaxation mode, recorded in the vicinity of 0.1 Hz, is influenced by interfacial polarization phenomena, which are strengthened in the case of the ternary system.

CONCLUSION

In this work, the water-mediated melt blending technique was employed to produce POM/CNF, POM/PU, and POM/PU/CNF systems using PU latex and aqueous CNF dispersion. The morphology, thermo-oxidative, mechanical (creep, stress relaxation, and tensile), and dielectric properties of the binary and ternary systems were studied. SEM proved a uniform distribution of the CNF in POM. The stiffness, strength, resistance to creep, and stress relaxation behaviors of POM were all improved, while the ductility reduced by CNF incorporation. Accordingly, CNF worked as a suitable nanoreinforcement in POM. CNF retained its reinforcing action when introduced into the POM/PU blend. The common use of PU and CNF in POM/PU/CNF resulted in a synergistic effect in respect to the thermo-oxidative stability. Finally, the dielectric behavior gave further insight in the variation of morphology of the related systems by considering the influence of interfacial polarization effects and changes in the relaxation transitions of the POM systems.

This work was performed in the framework of a bilateral collaboration between the Republic of South Africa and Hungary.

References

1. Plummer, C. J. G.; Scaramuzzino, P.; Kausch, H.-H.; Philippoz, J.-M. Polym Eng Sci 2000, 40, 1306.
2. Lesser, A. J Polym Eng Sci 1996, 36, 2366.
3. Plummer, C. J. G.; Menu, P.; Cudré-Mauroux, N.; Kausch, H.-H. J Appl Polym Sci 1995, 55, 489.
4. Xu, W.; He, P. J Appl Polym Sci 2001, 80, 304.
5. Mehrabzadeh, M.; Rezaie, D. J Appl Polym Sci 2002, 84, 2573.
6. Chiang, W. Y.; Huang, C. Y. J Appl Polym Sci 1993, 47, 105.
7. Siengchin, S.; Karger-Kocsis, J.; Psarras, G. C.; Thomann, R. J Appl Polym Sci 2008, 110, 1613.
8. Gao, X.; Qu, C.; Zhang, Q.; Peng, Y.; Fu, Q. Macromol Mater Eng 2004, 289, 41.
9. Sui, G.; Jana, S.; Zhong, W. H.; Fuqua, M. A.; Ulven, C. A. Acta Mater 2008, 56, 2381.
10. Sui, G.; Zhong, W. H.; Ren, X.; Wang, X. Q.; Yang, X. P. Mater Chem Phys 2009, 115, 404.

11. Prolongo, S. G.; Campo, M.; Gude, M. R.; Chaos-Morán, R.; Ureña, A. Compos Sci Technol 2009, 69, 349.
12. Karger-Kocsis, J. Express Polym Lett 2008, 2, 312.
13. Siengchin, S.; Karger-Kocsis, J.; Thomann, R. J Appl Polym Sci 2007, 105, 2963.
14. Siengchin, S.; Karger-Kocsis, J.; Thomann, R. Express Polym Lett 2008, 2, 746.
15. Shen, L.; Tjiu, W. C.; Liu, T. Polymer 2005, 46, 11969.
16. Hojfors, R. J.; Baer, E.; Geil, P. H. J Macromol Sci Phys 1977, 13, 323.
17. Shen, J.; Huang, W.; Wu, L.; Hu, Y.; Ye, M. Compos Sci Technol 2007, 67, 3041.
18. Tsangaris, G. M.; Psarras, G. C.; Kouloumbi, N. J Mater Sci 1998, 33, 2027.
19. Psarras, G. C.; Gatos, K. G.; Karahaliou, P. K.; Georga, S. N.; Krontiras, C. A.; Karger-Kocsis, J. Express Polym Lett 2007, 1, 837.
20. Sauer, B. B.; Avakian, P.; Flexman, E. A.; Keating, M.; Hsiao, B. S.; Verma, R. K. J Polym Sci Part B: Polym Phys 1997, 35, 2121.
21. Boyd, R. H. Polymer 1985, 26, 1123.
22. Hedvig, P. Dielectric Spectroscopy of Polymers; Adam Hilger: Bristol, 1977; p 283.
23. Tsangaris, G. M.; Psarras, G. C. J Mater Sci 1999, 34, 2151.
24. Gatos, K. G.; Martínez Alcázar, J. G.; Psarras, G. C.; Thomann, R.; Karger-Kocsis, J. Compos Sci Technol 2007, 67, 157.
25. Psarras, G. C.; Gatos, K. G.; Karger-Kocsis, J. J Appl Polym Sci 2007, 106, 1405.